

6. DATA REPORT: CALCIUM CARBONATE STRATIGRAPHY FROM SAMPLE MEASUREMENTS AND DIFFUSE SPECTRAL REFLECTANCE AT SITE 1090, ODP LEG 177¹

Suzanne O'Connell^{2,3} and Joseph Ortiz⁴

ABSTRACT

A total of 776 sediment samples were measured for percent CaCO₃ using a coulometer. These data are compared with percent blue reflectance (450–550 nm) measured with the Oregon State University split-core analysis track. In previous studies percent blue reflectance has been an excellent proxy for percent CaCO₃ and in this study shows many of the main depositional trends (i.e., a 100-k.y. cycle, with a 55% reflectance range evident in the upper 900 k.y., underlain by sediments exhibiting a 40-k.y. cycle with only a 30% reflectance range). Between ~21 and 5 Ma the average percent reflectance decreases from ~35% to ~8%. A similar decrease is also recorded between ~24 and 22 Ma.

Percent CaCO₃ trends closely match those of the percent blue spectral reflectance. This is especially well shown in the 100-k.y. cyclicity and in the interval between 24.5 and 21.5 Ma. In both intervals CaCO₃ analyses are abundant. An exception occurs in the interval between 2 and 5 meters composite depth (~193 and 240 k.y.). There, percent CaCO₃ and percent reflectance are out of phase. The lack of agreement is not likely to be due to a very wet core, in which water would dominate the spectral reflectance instead of sediment, or to problems with the composite depth slice. The discrepancy remains unexplained and provides clear evidence that when noninvasive measurements are used

¹O'Connell, S., and Ortiz, J., 2002. Data report: Calcium carbonate stratigraphy from sample measurements and diffuse spectral reflectance at Site 1090, ODP Leg 177. In Gersonde, R., Hodell, D.A., and Blum, P. (Eds.), *Proc. ODP, Sci. Results*, 177, 1–24 [Online]. Available from World Wide Web: <http://www-odp.tamu.edu/publications/177_SR/VOLUME/CHAPTERS/SR177_06.PDF>. [Cited YYYY-MM-DD]

²Department of Earth and Environmental Sciences, Wesleyan University, Middletown CT 06459, USA.

³Clement 107, Trinity College, 300 Summit Street, Hartford CT 06106, USA. soconnell@wesleyan.edu

⁴Lamont-Doherty Earth Observatory, Palisades, NY 10964, USA. Present address: Department of Geological Sciences, 221 McGilvrey Hall, Kent State University, Kent OH 44242, USA.

as proxies for chemical measurements they must be substantiated by the actual chemical or physical measurements.

INTRODUCTION

This paper examines the relationship between spectral reflectance and CaCO_3 measurements. There are two objectives for doing this. First, to see if spectral reflectance values can be used as a proxy for CaCO_3 measurements, and second, to see if paleoceanographic changes can be identified and studied using spectral measurement which are both quicker and cheaper to obtain than CaCO_3 measurements. This investigation was carried out on sediments from Site 1090.

Site 1090 ($42^{\circ}54.8'S$, $8^{\circ}55.2'E$) is located on the southern flank of the Agulhas Ridge in the central part of the Subantarctic Zone (Fig. F1). Although deep (3702 m of water), the site lies above the CaCO_3 compensation depth. It is near the present-day boundary between North Atlantic Deep Water (NADW, above) and Circumpolar Deep Water (CDW, below) (Fig. F2). Site 1090 is part of a three-site depth transect to intersect all of the major South Atlantic water masses. The other sites in this transect are Sites 1088 (2082 m) also on the Agulhas Ridge and Site 1089 (4620 m) in the Cape Basin.

Site 1090 was drilled to recover upper Miocene to Pleistocene sediments to investigate changes in the location of the Polar Front Zone, investigate changes in the mixing ratios of CDW and NADW, and investigate the response of the Southern Ocean to orbital forcing. In particular, it was hoped that this site would provide sediments that would allow the examination of phase relationships to climatic changes identified in the Northern Hemisphere.

Five holes were drilled, reaching a maximum depth of 397.5 meters below seafloor (mbsf) and middle Eocene age (~46 Ma). The Quaternary sediments consist of alternating foraminifer nannofossil ooze, diatom-bearing nannofossil ooze, and mud-bearing nannofossil ooze with several short hiatuses. A Miocene through early Pliocene hiatus, extending over 10 m.y. is marked by a lithologic change with white nannofossil ooze above and reddish, mud-rich nannofossil ooze below. Miocene and Oligocene sediments consist of mud-bearing diatom ooze and mud- and diatom-bearing nannofossil ooze and chalk. Opal-rich sediments dominate the upper Eocene interval, whereas calcareous sediments predominate in the middle Eocene sediments (Fig. F2). Here we present data comparing spectral reflectance and percent CaCO_3 .

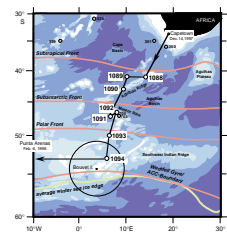
METHODS AND DATA

All values are given in meters composite depth (mcd) or age. Depths given are from the top of the sampled interval. Composite depths are those determined by the Leg 177 Shipboard Party (Gersonde, Hodell, Blum, et al., 1999).

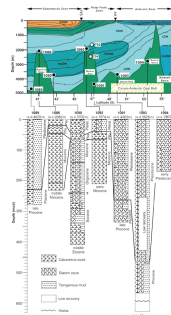
AGE MODEL

The age model is based on biostratigraphic and paleomagnetic shipboard age picks published in the Leg 177 *Initial Reports* volume (Gersonde, Hodell, Blum, et al., 1999) and used to calculate sedimentation

F1. Leg 177 site location map, p. 8.



F2. Cross-section of Leg 177 transect, p. 9.



rates (Fig. F3; Table T1). Sedimentation rates were generally higher in the Quaternary, averaging almost 2 cm/k.y., but ranging from <1 to >6 cm/k.y. Below the hiatus (~70 mcd), sedimentation rates were considerably lower, averaging slightly >1 cm/k.y.

Ages from the shipboard age model were used in the program AGER developed by Philip Howell (pers. comm., 1999) at Brown University to assign ages to data presented in this paper.

BULK DENSITY

Bulk density measurements are compared with CaCO_3 and spectral values. Bulk density was determined with the shipboard gamma ray attenuation (GRA) densitometer (Gersonde, Hodell, Blum, et al., 1999). In this study, the raw data were evaluated hole by hole. Adjacent measurements differing by more than ~8% in a single hole were eliminated. Then all Site 1090 data were combined and sorted by meters composite depth. A five-point running average was used to smooth the data (Table T2). The measurements are shown plotted vs. depth and weight percent CaCO_3 in Figure F4A and F4B. The weight percent CaCO_3 values roughly parallel the bulk density values.

MOISTURE AND DENSITY

Moisture and density measurements were made during Leg 177 on selected samples at a rate of about one per core section following the procedures outlined in *ODP Technical Note 26* (Blum, 1997). Samples were dried for 24 hr either in an oven at temperatures of 105°C or in a freeze-dryer.

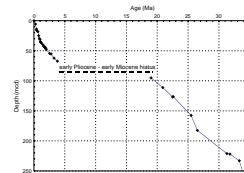
Dry density and water content data are given in Table T3 and plotted vs. depth in Figure F5A (0–250 mcd). These two parameters are inversely related, which is expected because they are both directly related to the dry mass of the solids (Blum, 1997). Plotting dry density and weight percent CaCO_3 vs. depth, shows no relationship between the two measurements (Fig. F5B, F5C).

DIFFUSE SPECTRAL REFLECTANCE

Diffuse spectral reflectance measurements were made with the Oregon State University split-core analysis track (SCAT). This instrument or its prototype has been used to measure reflectance sediments during Leg 138 (Mix et al., 1992, 1995), Leg 154 (Harris et al., 1997; Harris and Mix, 1999), and Leg 162 (Ortiz et al., 1999) sediments. The instrument measures light reflected from split sediment core surfaces at a spectral resolution of 0.68 nm and spans wavelengths from 250 to 950 nm, thereby including the upper ultraviolet (UV), visible, and near-infrared wavelengths. The core is illuminated via a fiber-optic cable by two light sources, a deuterium lamp for the UV and a quartz-tungsten-halogen lamp for the visible and near-infrared (nIr) wavelengths.

During Leg 177, closely spaced measurements were converted to percent reflectance and averaged into four 100-nm-wide bands defined as (1) UV (250–350 nm), (2) blue (450–550 nm), (3) red (650–750 nm), and (4) nIr (850–950 nm) (Table T4). The signal is most reproducible in the red and blue wavelengths. Although values for these two wavelengths

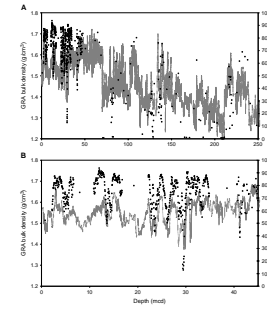
F3. Sedimentation rate based on Leg 177 shipboard age determinations, p. 10.



T1. Shipboard age determinations used to calculate sedimentation rates, p. 18.

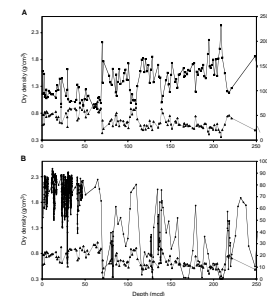
T2. Original and average shipboard GRA bulk density values, p. 19.

F4. Averaged GRA bulk density and weight percent CaCO_3 vs. depth, p. 11.



T3. Shipboard dry density and water content values made on selected sediment core samples, p. 20.

F5. Averaged dry density vs. dry water content for Site 1090 and averaged dry density and weight percent CaCO_3 vs. depth, p. 12.



have similar trends, they do show variations attributed to different components of the sediment (Fig. F6). The blue band is used for comparison to the CaCO_3 content of sediments because calcite has a somewhat higher reflectance at this wavelength than at longer wavelengths. Because of this, percent blue reflectance should be a better proxy for CaCO_3 (see Mix et al., 1995) (Figs. F7, F8).

CALCIUM CARBONATE

The CaCO_3 content of the sediment column is a function of production, dissolution, and dilution. In ocean cores carbonate content closely parallels oxygen isotope stratigraphy and has been widely used for stratigraphic correlation and to interpret paleoceanographic changes (e.g., Hayes et al., 1969; Prell, 1978; Dunn et al., 1981; Gardner, 1982; Pisias et al., 1985; O'Connell, 1990).

A total of 776 CaCO_3 analyses is available for Site 1090, including 80 shipboard analyses on Hole 1090B (Table T5). The remaining analyses were done on samples from Holes 1090D and 1090E.

Samples were dried in a freeze-dryer, powdered, weighed to the nearest milligram, and analyzed for CaCO_3 using a Coulometrics CO_2 coulometer. The coulometer has an accuracy of 0.15% (± 0.2 mg). The coulometric titration technique measures all of the CO_2 that is liberated by acidifying and heating sediment samples in a closed system. To do this, the powdered samples are placed in a test tube that is attached to the coulometer, placed in a heat shield, and 2-N HCl is pumped into the test tube. The liberated CO_2 is transferred through scrubbers (solutions to remove interfering substances) by a CO_2 -free gas into an absorption cell, where it is titrated through coulometric means. The absorption cell contains an aqueous medium of ethanolamine and a coulometric indicator. The interaction of the CO_2 and the cell solution creates a titratable acid. The coulometer forms a base electrically and titrates to an end point determined by the optical transmission of the indicator (Huffman, 1977). The pulse output was scaled and fed to a counter in terms of CO_2 . A stable coulometer reading indicates that all of the CO_2 has been evolved and titrated. The reading was recorded and the results were calculated in micrograms carbon and CaCO_3 (weight percent CaCO_3 = percent C_{inorg} $\times 8.334$). This method of calculation assumes that all of the CO_2 is liberated from CaCO_3 .

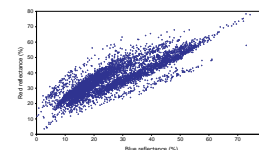
DISCUSSION

The percent blue band reflectance varies from 0% to 70% and shows several trends. The consistently highest values (15% to 70%) and those with the most variation (55% reflectance range) are between 0 and 30 mcd corresponding to ~ 0.9 m.y. (Figs. F7A, F8A, F8B). In most marine sediments, this Quaternary interval shows a strong 100-k.y. Milankovitch cycle. Although the possibility of such a cycle is visible in this record, it does not stand out. This may be caused by problems with the age model. Carbonate values in this interval range from ~10% to 75% and with the exception of the interval between 2 and 5 mcd, parallel the blue spectral reflectance values.

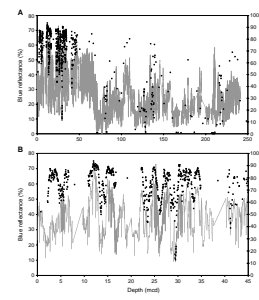
Between 2 and 5 mcd percent blue reflectance and percent CaCO_3 are out of phase. This could be due to a very wet core, but this is not likely

T4. Shipboard spectral reflectance values given as percent reflectance in 100-nm intervals, p. 23.

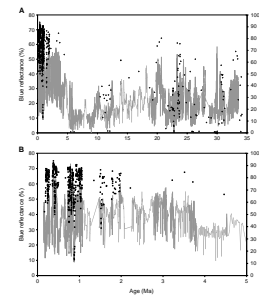
F6. Percent blue reflectance vs. percent red reflectance, p. 14.



F7. Percent blue reflectance and weight percent CaCO_3 vs. depth, p. 15.



F8. Percent blue reflectance and percent CaCO_3 vs. age and weight percent red reflectance and percent CaCO_3 vs. age, p. 16.



T5. Weight percent CaCO_3 values, p. 24.

as water content values for this interval measured for Holes 1090A and 1090B are similar to water content values in the rest of the core (Figs. F4, F5; Tables T2, T3). By contrast, the percent carbonate values do show roughly the same trend as the GRA bulk density values (Fig. F4B). Alternatively, because water content and spectral reflectance were measured on samples from Hole 1090A, and the carbonate measurements were made on samples from Hole 1090D, it is possible that there is a problem with the composite splice. However, this is also not likely because the shipboard carbonate measurements, made on samples from Hole 1090B, are in agreement with the shore-based measurements made on samples from Hole 1090D. Thus, at this time there is no explanation for the discrepancy between carbonate and spectral reflectance between 2 and 5 mcd.

Between ~30 and 65 mcd (~0.9 and 3.8 m.y.), the range of variation in percent blue reflectance decreases (20% to 55%) and the cycles are much shorter (Fig. F8B), probably corresponding to the 40-k.y. Milankovitch cycle. Each of these cycles is defined by a sharp decrease in percent blue reflectance to close to 20%, with the rest of the cycle being above 40%. Similar cycles identified by a decrease on g/cm^3 are also observed in the GRA bulk density measurements (Fig. F4A).

Below ~70 mcd, both the percent blue reflectance values and the GRA bulk density values decrease sharply (Figs. F4A, F7A). This corresponds to the lower Pliocene–lower Miocene hiatus. Percent CaCO_3 measurements in this interval are scarce. However, those that are available correlate well with the percent blue reflectance.

In the remaining core, both the percent blue reflectance values and the GRA bulk density values continue to show similar trends, although the detail and magnitude of the changes are different. Below ~160 mcd, when very low percent CaCO_3 values (~1%) are encountered, the percent blue reflectance does not indicate as much of a decrease, having values of over 15%. This is in contrast to the very low carbonate values encountered just below the lower Pliocene–lower Miocene hiatus, where percent blue reflectance values were <5%. This is the opposite of the correlation between the low percent carbonate measurements with the GRA bulk density values. The low carbonate correlation is much better in the older sediments (210 mcd) than at the hiatus at 70 mcd (Fig. F4A).

CONCLUSIONS

Diffuse spectral reflectance, both blue and red, is a good proxy for CaCO_3 in these three-component (carbonate, biogenic silica, and terrigenous) Antarctic sediments.

The out-of-phase relationship between CaCO_3 and diffuse spectral reflectance between 2 and 5 mcd cannot be explained at this time.

ACKNOWLEDGMENTS

We thank ODP and the curators at the German ODP Core Repository for samples. We thank our Leg 177 scientific and technician colleagues and the crew of the *JOIDES Resolution* for collecting the cores. We also thank Amanda Long and Daniel King for generating the carbonate analyses. The authors thank Brandon Dugan for his thoughtful review.

This research used samples and data provided by the Ocean Drilling Program (ODP). ODP is sponsored by the U.S. National Science Foundation (NSF) and participating countries under management of Joint Oceanographic Institutions (JOI), Inc. Funding for the research was provided by USSAC grant numbers USSSP F000851 to J. Ortiz and USSSP F000986 to Suzanne O'Connell.

REFERENCES

- Blum, P., 1997. Physical properties handbook: a guide to the shipboard measurement of physical properties of deep-sea cores. *ODP Tech. Note*, 26 [Online]. Available from World Wide Web: <<http://www-odp.tamu.edu/publications/tnotes/tn26/INDEX.HTM>>. [Cited 2001-09-20]
- Dunn, D.A., Moore, T.C., and Keigwin, L.D., 1981. Atlantic-type carbonate stratigraphy in the late Miocene Pacific. *Nature*, 291:227.
- Gardner, J.V., 1982. High-resolution carbonate and organic-carbon stratigraphies for the late Neogene and Quaternary from the western Caribbean and eastern equatorial Pacific. In Prell, W.L., Gardner, J.V., et al., *Init. Repts. DSDP*, 68: Washington (U.S. Govt. Printing Office), 347–364.
- Gersonde, R., Hodell, D.A., Blum, P., et al., 1999. *Proc. ODP, Init. Repts.*, 177 [CD-ROM]. Available from: Ocean Drilling Program, Texas A&M University, College Station, TX 77845-9547, U.S.A.
- Harris, S.E., and Mix, A.C., 1999. Pleistocene precipitation balance in the Amazon Basin recorded in deep-sea sediments. *Quat. Res.*, 51:14–26.
- Harris, S.E., Mix, A.C., and King, T., 1997. Biogenic and terrigenous sedimentation at Ceara Rise, western tropical Atlantic, supports Pliocene–Pleistocene deep-water linkage between hemispheres. In Shackleton, N.J., Curry, W.B., Richter, C., and Bralower, T.J. (Eds.), *Proc. ODP, Sci. Results*, 154: College Station, TX (Ocean Drilling Program), 331–345.
- Hays, J.D., Saito, T., Opdyke, N.D., and Burckle, L.H., 1969. Pliocene-Pleistocene sediments of the equatorial Pacific: their paleomagnetic, biostratigraphic, and climatic record. *Geol. Soc. Am. Bull.*, 80:1481–1513.
- Huffman, E.W.D., 1977. Performance of a new automatic carbon dioxide coulometer. *Microchem. J.*, 22:567–573.
- Mix, A.C., Harris, S.E., and Janecek, T.R., 1995. Estimating lithology from noninvasive reflectance spectra: Leg 138. In Pisias, N.G., Mayer, L.A., Janecek, T.R., Palmer-Julson, A., and van Andel, T.H. (Eds.), *Proc. ODP, Sci. Results*, 138: College Station, TX (Ocean Drilling Program), 413–427.
- Mix, A.C., Rugh, W., Pisias, N.G., Veirs, S., Leg 138 Shipboard Sedimentologists (Hagelberg, T., Hovan, S., Kemp, A., Leinen, M., Levitan, M., Ravelo, C.), and Leg 138 Scientific Party, 1992. Color reflectance spectroscopy: a tool for rapid characterization of deep-sea sediments. In Mayer, L., Pisias, N., Janecek, T., et al., *Proc. ODP, Init. Repts.*, 138 (Pt. 1): College Station, TX (Ocean Drilling Program), 67–77.
- O'Connell, S.B., 1990. Variations in Upper Cretaceous and Cenozoic calcium carbonate percentages, Maud Rise, Weddell Sea, Antarctica. In Barker, P.F., Kennett, J.P., et al., *Proc. ODP, Sci. Results*, 113: College Station, TX (Ocean Drilling Program), 971–984.
- Ortiz, J., Mix, A.C., Harris, S., and O'Connell, S., 1999. Diffuse spectral reflectance as a proxy for percent carbonate content in North Atlantic sediments. *Paleoceanography*, 14:171–186.
- Pisias, N.G., Shackleton, N.J., and Hall, M.A., 1985. Stable isotope and calcium carbonate records from hydraulic piston cored Hole 574A: high-resolution records from the middle Miocene. In Mayer, L., Theyer, F., Thomas, E., et al., *Init. Repts. DSDP*, 85: Washington (U.S. Govt. Printing Office), 735–748.
- Prell, W.L., 1978. Upper Quaternary sediments of the Colombia Basin: spatial and stratigraphic variations. *Geol. Soc. Am. Bull.*, 89:1241–1255.

Figure F1. Leg 177 site location map (from Gersonne, Hodell, Blum, et al., 1999).

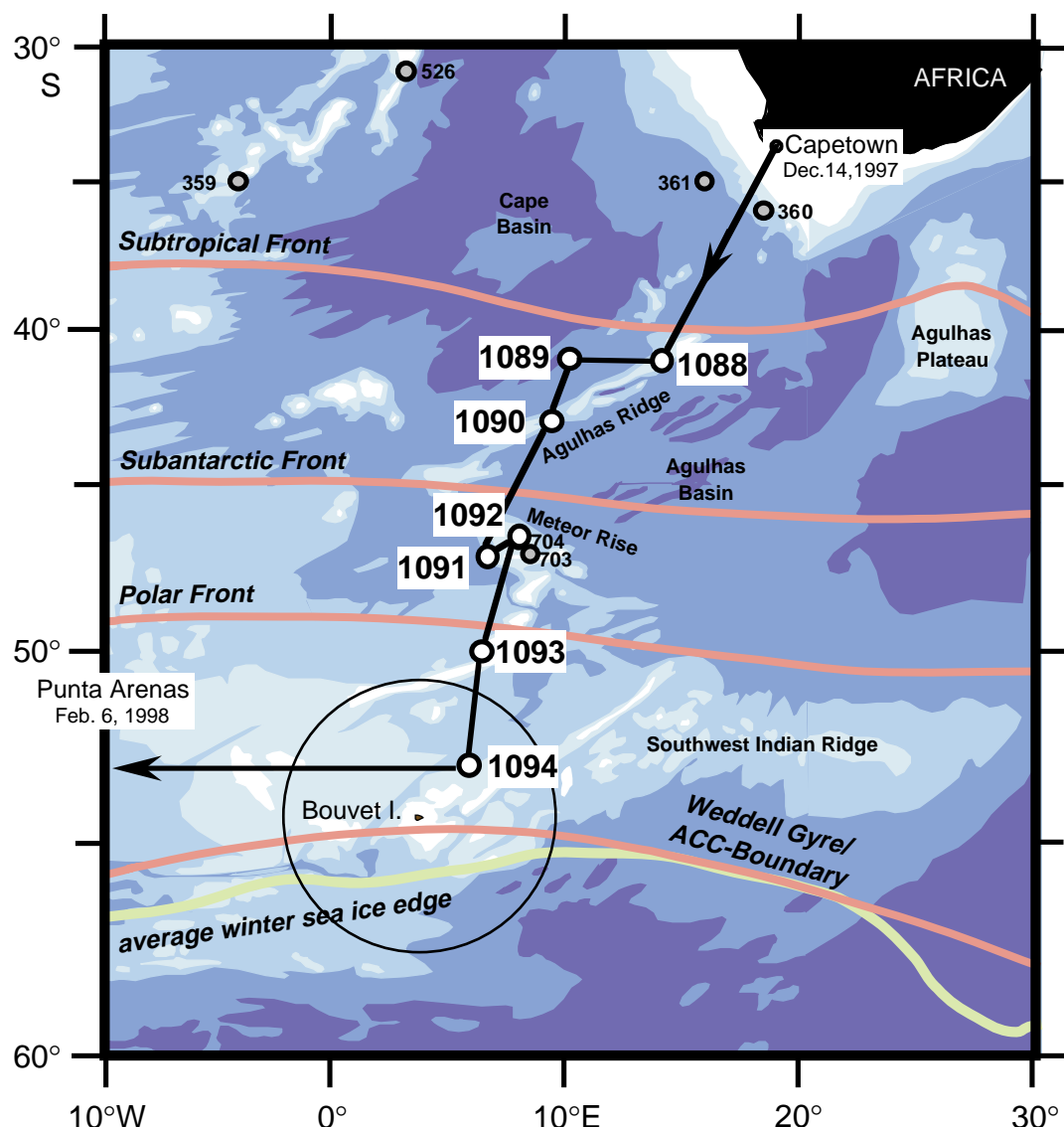


Figure F2. Cross-section of Leg 177 transect (see Fig. F1, p. 8) showing site locations, water mass structure and topography (top), and lithologic summary of the eight sites cored during Leg 177 (bottom) (from Geronde, Hodell, Blum, et al., 1999). NADW = North Atlantic Deep Water, CDW = Circumpolar Deep Water, AABW = Antarctic Bottom Water, AAIW = Antarctic Intermediate Water, SASW = Subantarctic Surface Water, SAF = Subantarctic Front, PF = Polar Front. w.d. = water depth.

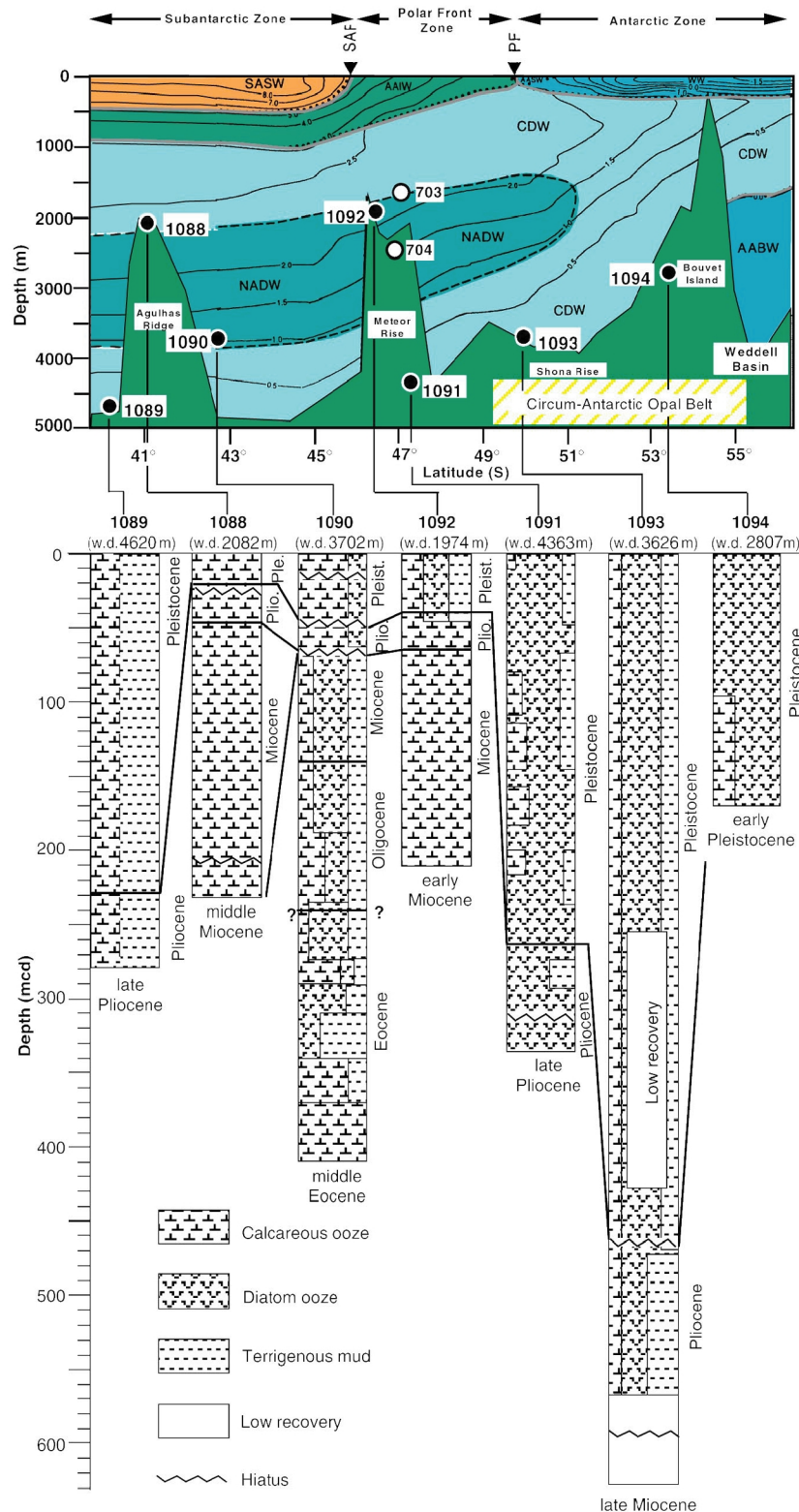


Figure F3. Sedimentation rate based on Leg 177 shipboard age determinations (from Gersonde, Hodell, Blum, et al., 1999).

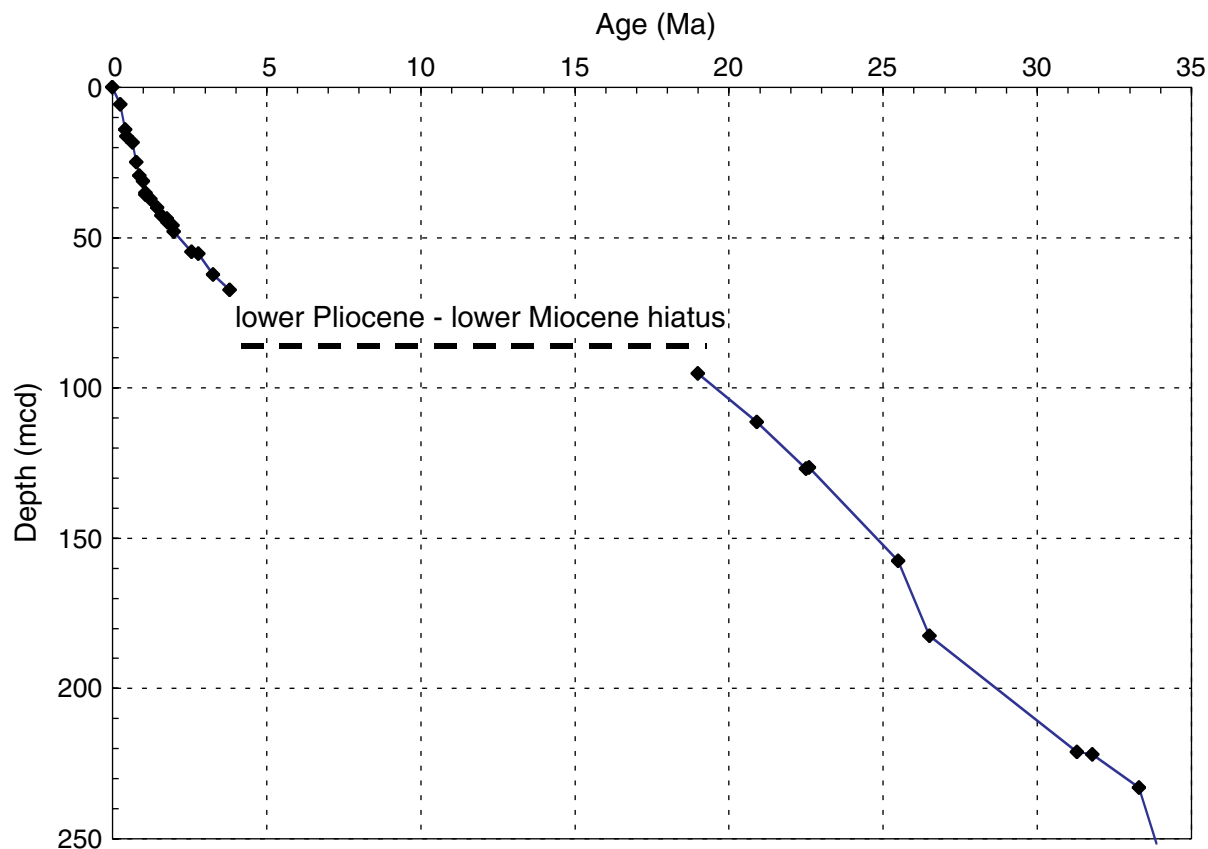


Figure F4. Averaged shipboard GRA bulk density (solid line) values (from Gersonde, Hodell, Blum, et al., 1999) and weight percent CaCO_3 (dots) vs. depth. A. 0–250 mcd. B. 0–45 mcd.

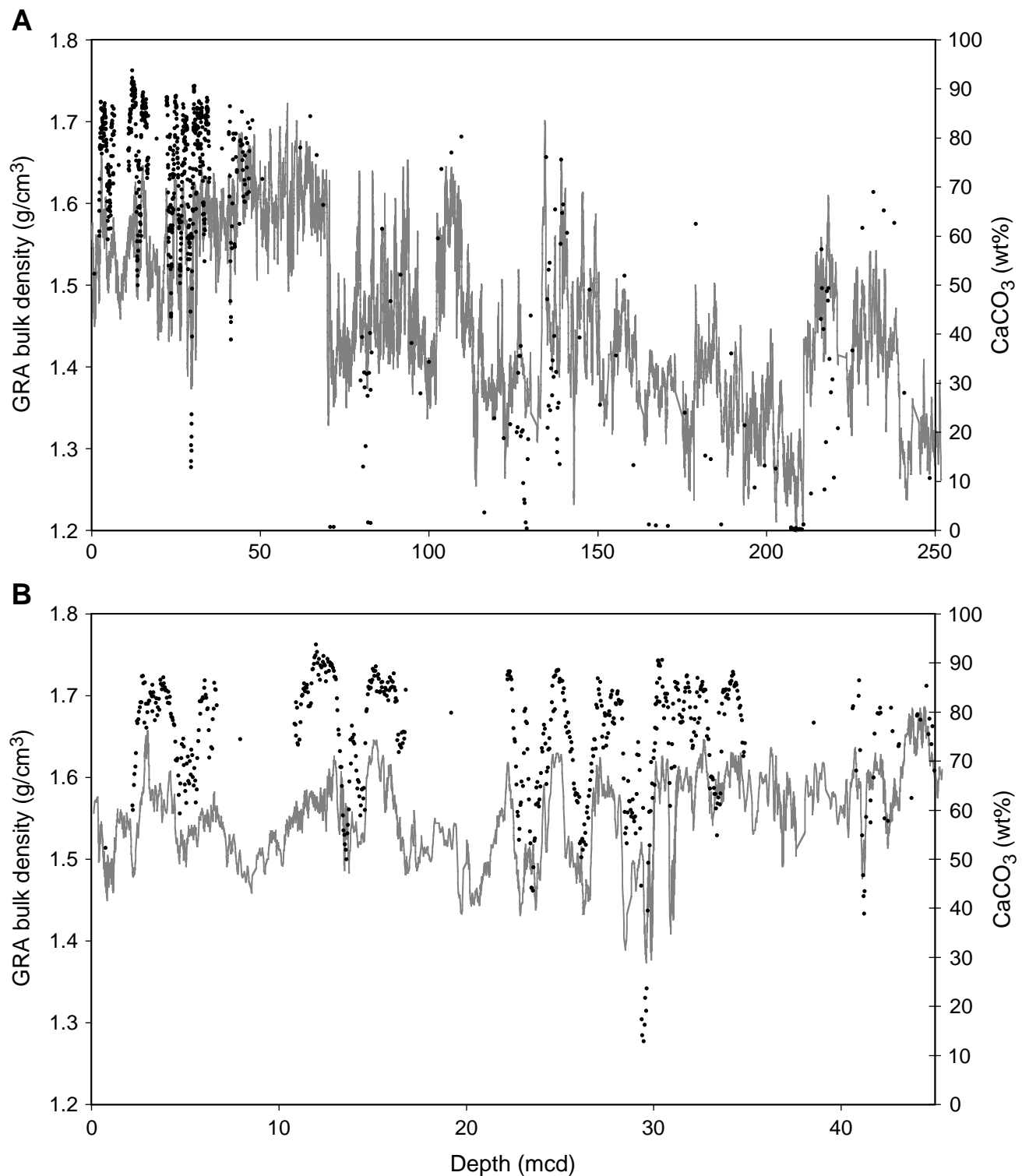


Figure F5. A. Averaged dry density (triangles) vs. dry water content (dots) for Site 1090. B. Averaged dry density (triangles) and weight percent CaCO_3 (dots) vs. depth for 0–250 mcd. (Continued on next page.)

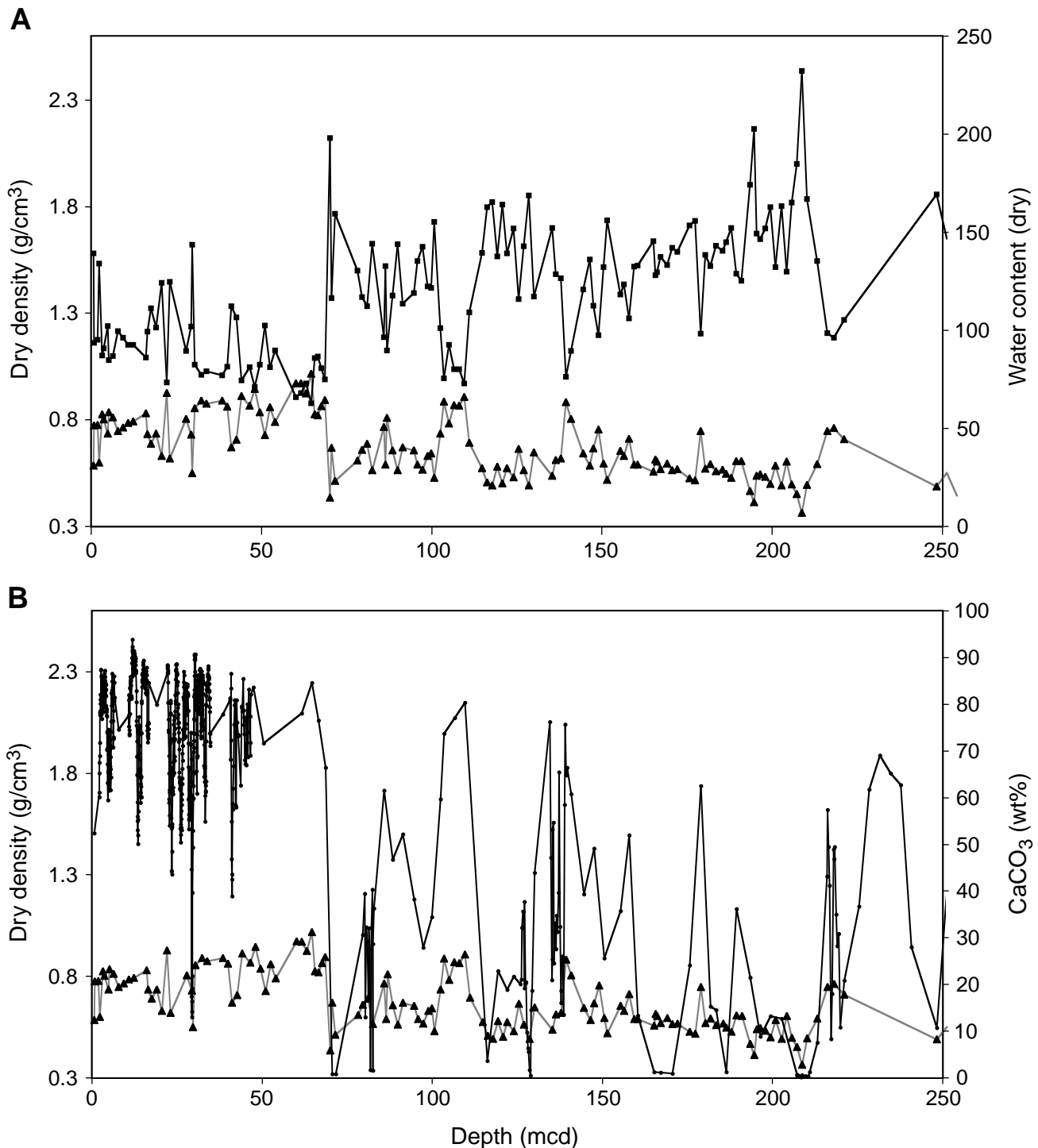


Figure F5 (continued). C. Averaged dry density (triangles) and weight percent CaCO_3 (dots) vs. depth for 0–45 mcd.

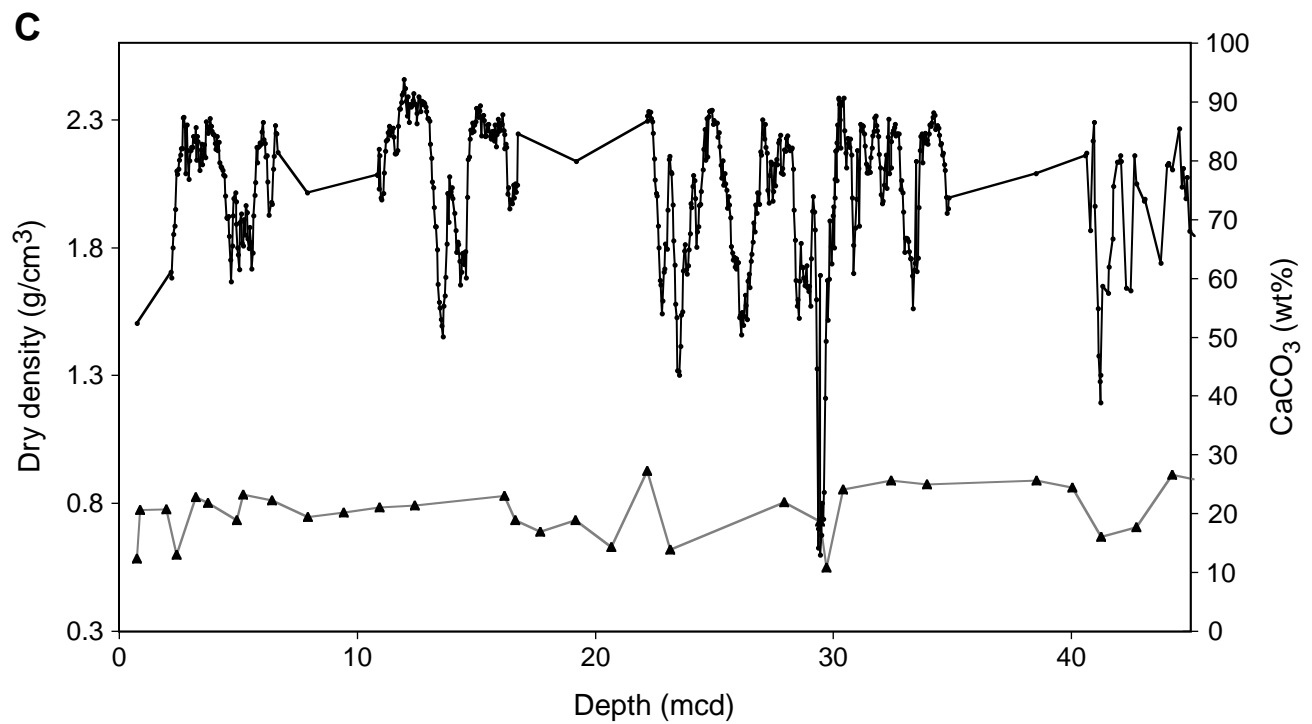


Figure F6. Percent blue reflectance (450–550 nm) vs. percent red reflectance (650–750 nm) (from Gersonde, Hodell, Blum, et al., 1999).

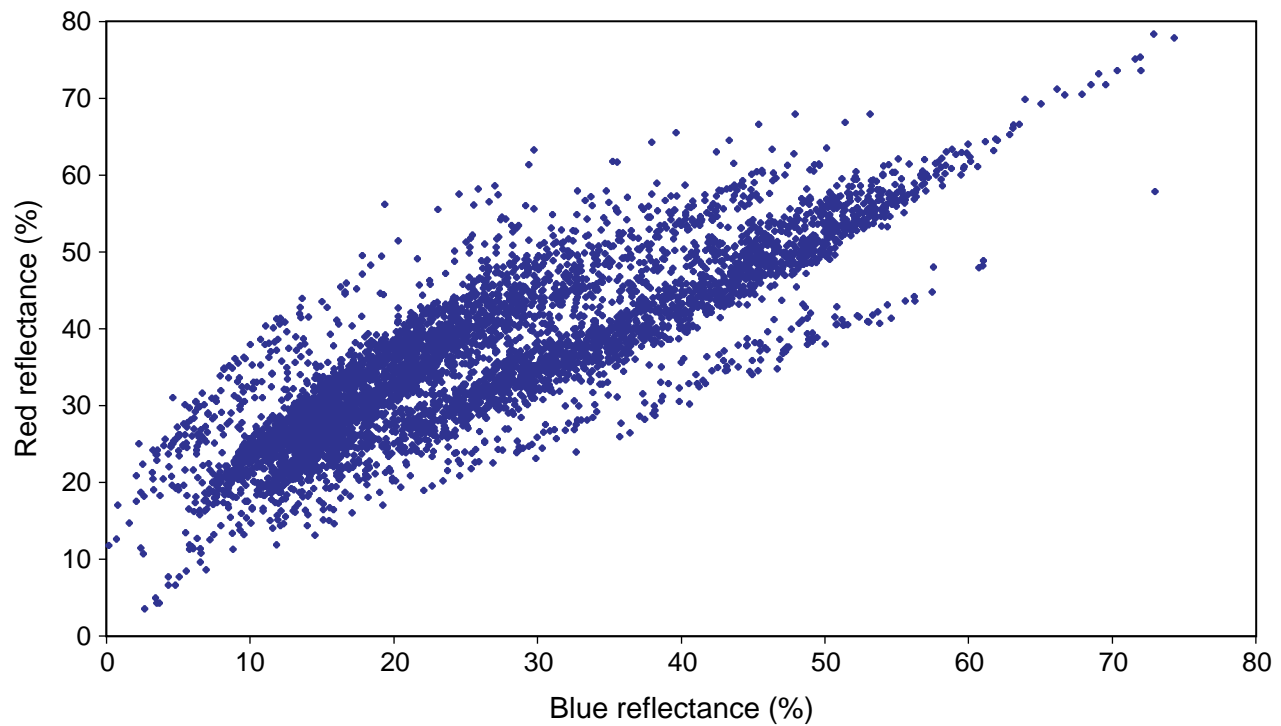


Figure F7. Percent blue reflectance (450–550 nm) (solid line) and weight percent CaCO_3 (dots) vs. depth.
A. 0–250 mcd. **B.** 0–45 mcd.

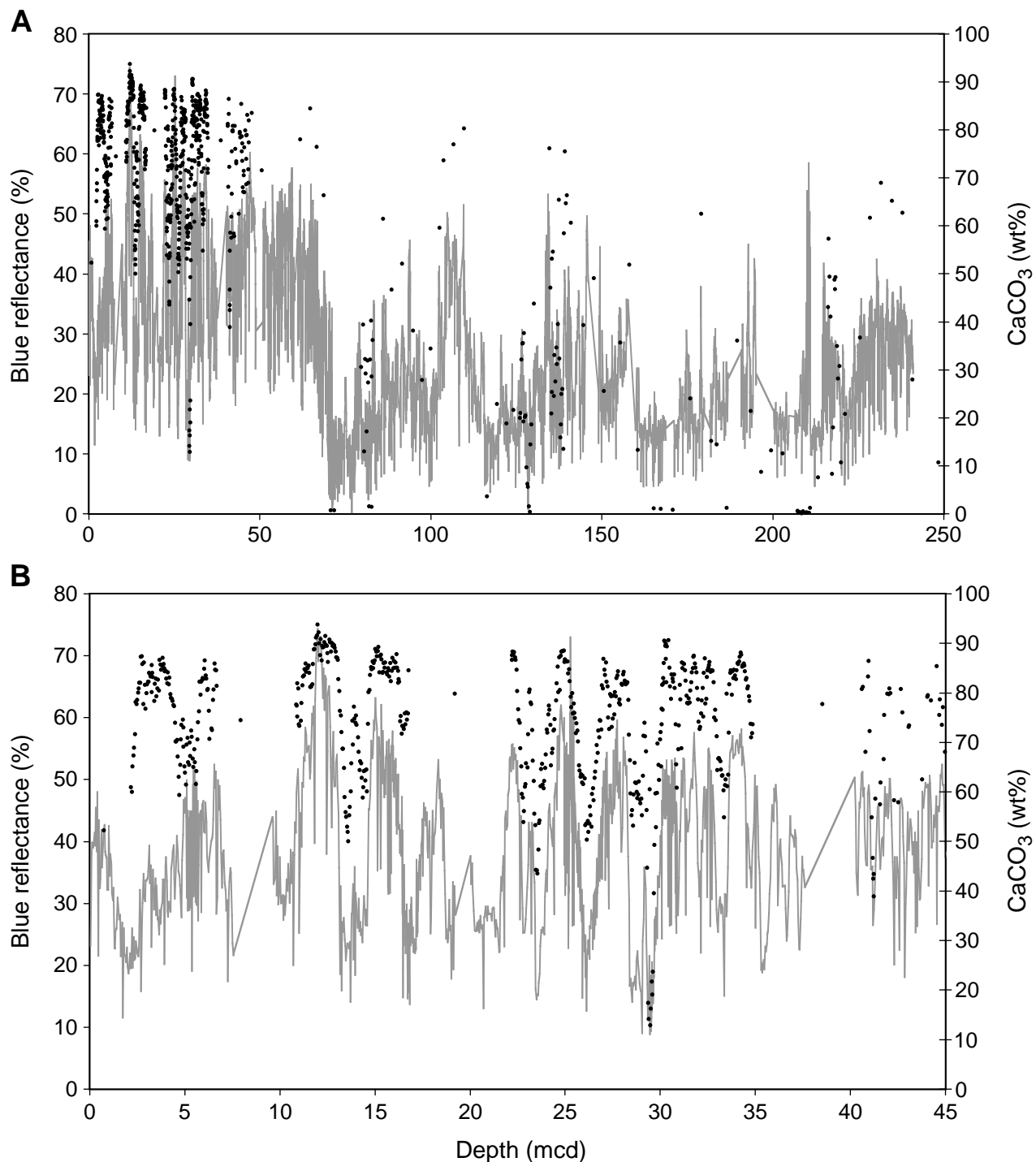


Figure F8. Percent blue reflectance (450–550 nm) and weight percent CaCO_3 vs. age. A. 0–35 Ma. B. 0–5 Ma. (Continued on next page.)

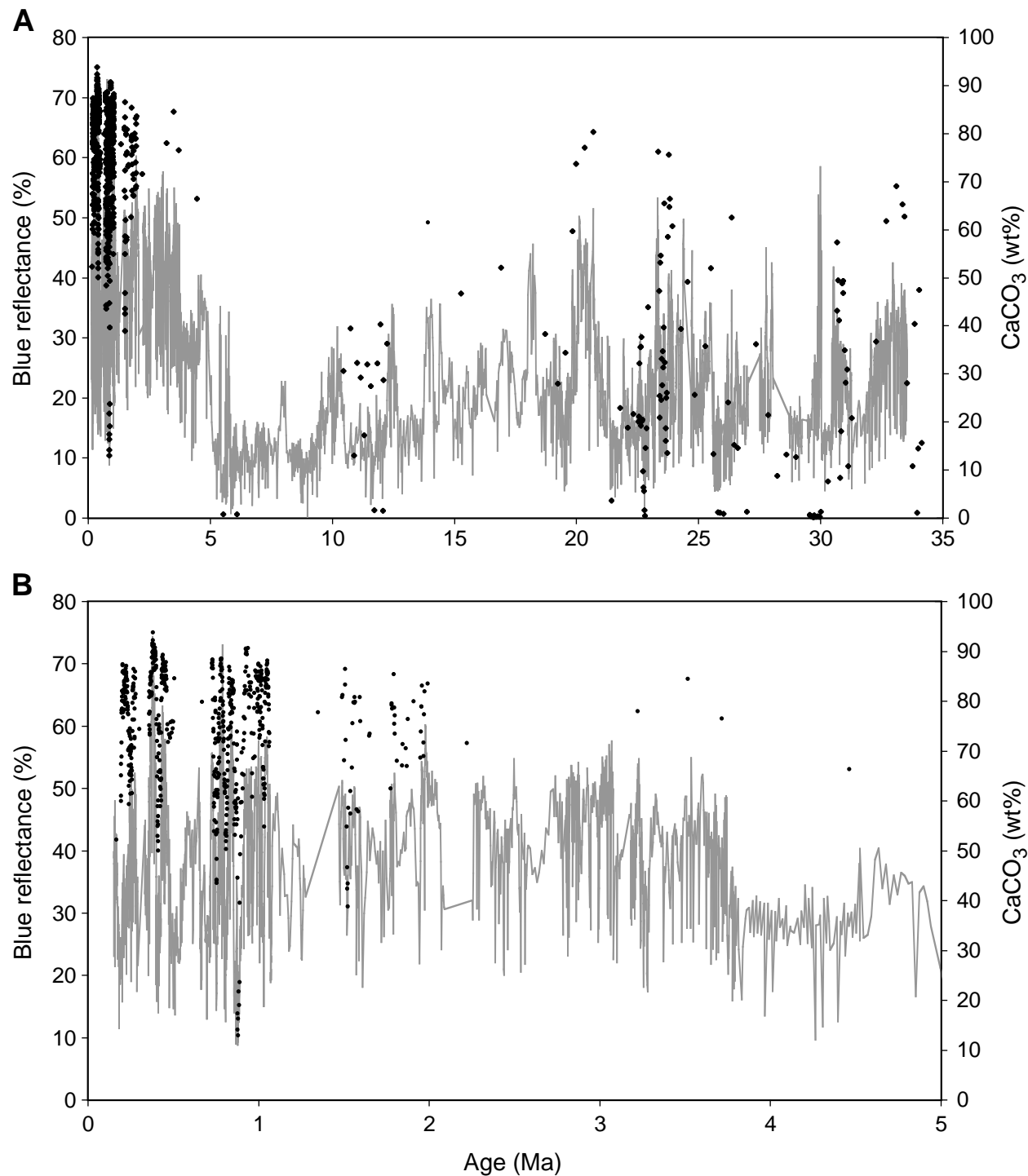


Figure F8 (continued). C. Percent blue reflectance (450–550 nm) and weight percent CaCO_3 vs. age for 0–1 Ma. **D.** Percent red reflectance (650–750 nm) and weight percent CaCO_3 vs. age for 0–1 Ma.

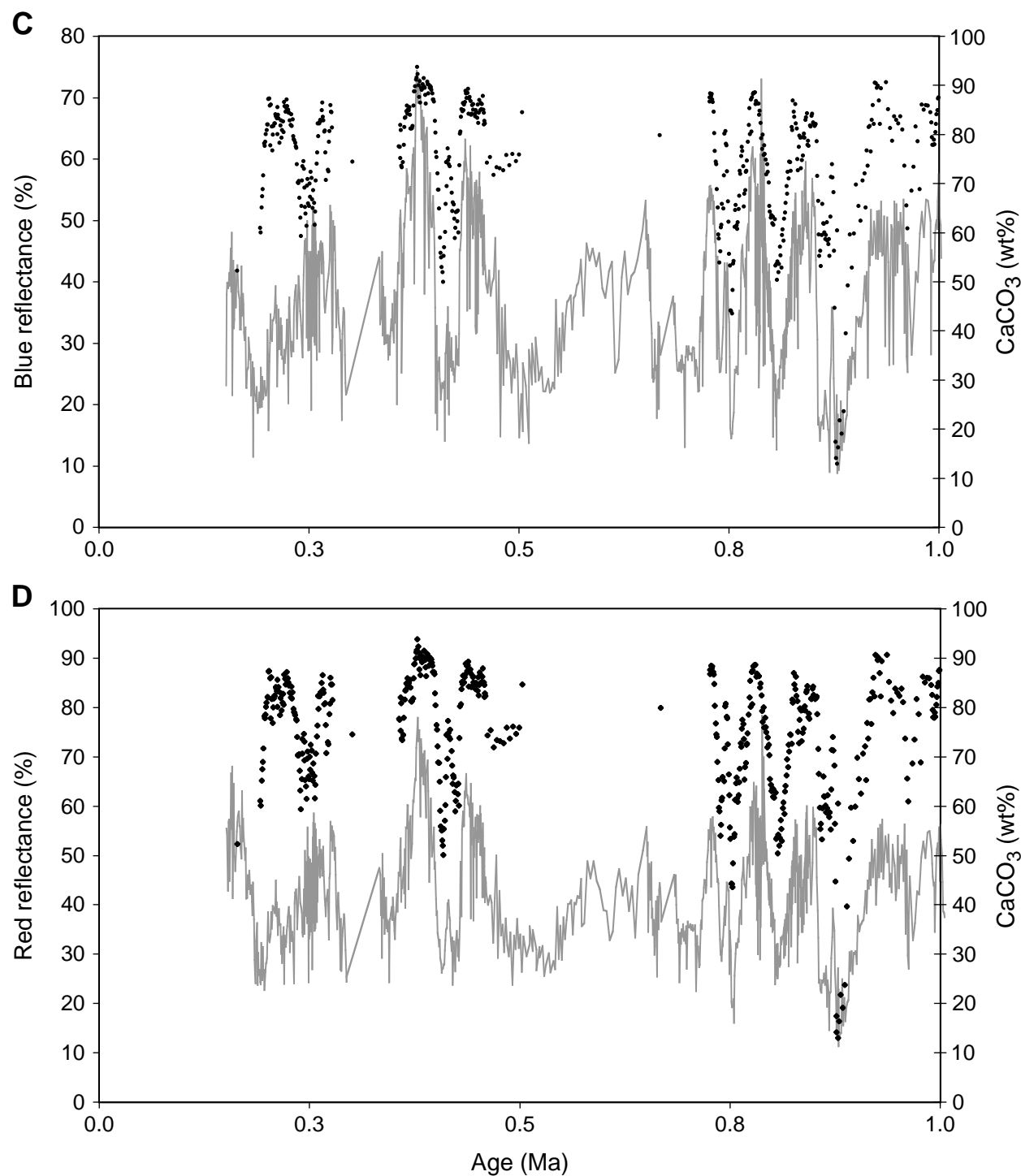


Table T1. Shipboard age determinations used to calculate sedimentation rates.

Age (Ma)	Depth (mbsf)	Depth (mcd)	Code	Event abbreviation	Event/Zone/Chron	Sedimentation rates (cm/k.y.)
0.26	5.75	5.75	CN	FO	<i>E. huxleyi</i>	2.21
0.42	12.35	14.15	DIAT	BOT	<i>T. lentiginosa</i> Subzone b	5.25
0.46	14.55	16.3	CN	LO	<i>P. lacunosa</i>	5.38
0.65	15.43	18.3	DIAT	TOP	<i>A. ingens</i> Subzone c	1.05
0.78	18.6	24.89	PMAG	BOT	C1n (Brunhes)	5.07
0.88	27	29.51	CN	LO	<i>R. asanoi</i>	4.62
0.99	25	31.31	PMAG	TOP	C1r.1n (Jaramillo)	1.64
1.07	28.05	35.23	PMAG	BOT	C1r.1n (Jaramillo)	4.90
1.08	32.78	35.84	CN	FO	<i>R. asanoi</i>	6.10
1.24	33.53	37.14	CN	LO	Geph. large (>5.5 µm)	0.81
1.46	36.71	40.01	CN	FO	Geph. large (>5.5 µm)	1.30
1.60	39.65	42.81	CN	LO	<i>C. macintyrei</i>	2.00
1.77	35.65	43.7	PMAG	TOP	C2n (Olduvai)	0.52
1.80	41.45	44.91	DIAT	TOP	<i>P. barboi</i> Zone	4.03
1.95	37.9	45.95	PMAG	BOT	C2n (Olduvai)	0.69
2.00	39.8	47.97	DIAT	TOP	<i>T. kolbei</i> - <i>F. matuyamae</i> Z.	4.04
2.58	46.9	54.72	PMAG	BOT	C2r (Matuyama)	1.16
2.80	50.37	55.38	DIAT	TOP	<i>T. insignia</i> Subzone a	0.30
3.26	54.15	62.32	DIAT	TOP	<i>F. interfrigidara</i> Zone	1.51
3.80	63.9	67.46	DIAT	BOT	<i>F. interfrigidara</i> Zone	0.95
19.00	85.15	95.29	DIAT	LO	<i>T. spumellaroides</i>	hiatus
20.90	101.9	111.41	DIAT	BOT	<i>T. fraga</i> Zone	0.85
22.60	116.9	126.51	DIAT	BOT	<i>T. spumellaroides</i> Zone	0.89
25.50	150.56	157.63	DIAT	LO	<i>R. vigilans</i>	1.07
26.50	174.9	182.59	DIAT	BOT	<i>R. gelida</i> Zone	2.50
31.30	213.9	221.2	CN	LO	<i>R. umbilica</i>	0.80
31.80	214.08	221.93	CN	LO	<i>I. recurvus</i>	0.15
33.30	221.1	232.06	CN	Acme	<i>Clausicoccus</i> spp.	0.68
34.20	250.1	262.09	CN	LO	<i>D. saipanensis</i>	3.34
36.00	289.5	301.49	CN	FO	<i>I. recurvus</i>	2.19
38.00	349.12	361.11	CN	FO	<i>R. bisecta</i>	2.98
43.10	372.58	384.57	CN	LO	<i>Nannotetridina</i> spp.	0.46

Notes: Code abbreviations: DIAT = diatom, CN = calcareous nannofossil, PMAG = magnetic polarity, RAD = radiolarians. Event abbreviations: FO = first occurrence, LO = last occurrence, RE = reentrance, TOP = top of zone, BOT = bottom of zone. Shipboard age determinations taken from Gersonde, Hodell, Blum, et al., 1999.

Table T2. Original and averaged shipboard GRA bulk density values.

Leg	Site	Hole	Core	Type	Section	Top (cm)	Depth (mbsf)	Depth (mcd)	GRA bulk density (g/cm ³)	GRA bulk density, 5-pt average (g/cm ³)
177	1090	B	1	H	1	10	0.1	0.1	1.538	
177	1090	B	1	H	1	12	0.12	0.12	1.546	
177	1090	B	1	H	1	14	0.14	0.14	1.567	1.5558
177	1090	B	1	H	1	16	0.16	0.16	1.562	1.564
177	1090	B	1	H	1	18	0.18	0.18	1.566	1.57
177	1090	B	1	H	1	20	0.2	0.2	1.579	1.57
177	1090	B	1	H	1	22	0.22	0.22	1.576	1.5716
177	1090	B	1	H	1	24	0.24	0.24	1.567	1.5722
177	1090	B	1	H	1	26	0.26	0.26	1.570	1.5714
177	1090	B	1	H	1	28	0.28	0.28	1.569	1.5696
177	1090	B	1	H	1	30	0.3	0.3	1.575	1.573
177	1090	B	1	H	1	32	0.32	0.32	1.567	1.5752
177	1090	B	1	H	1	34	0.34	0.34	1.584	1.5756
177	1090	B	1	H	1	36	0.36	0.36	1.581	1.5476
177	1090	B	1	H	1	38	0.38	0.38	1.571	1.5508
177	1090	D	1	H	1	4	0.04	0.38	1.435	1.5212
177	1090	B	1	H	1	40	0.4	0.4	1.583	1.5196
177	1090	D	1	H	1	6	0.06	0.4	1.436	1.4964
177	1090	B	1	H	1	42	0.42	0.42	1.573	1.5248
177	1090	D	1	H	1	8	0.08	0.42	1.455	1.4984
177	1090	B	1	H	1	44	0.44	0.44	1.577	1.5296
177	1090	D	1	H	1	10	0.1	0.44	1.451	1.5108
177	1090	B	1	H	1	46	0.46	0.46	1.592	1.5318
177	1090	D	1	H	1	12	0.12	0.46	1.479	1.5202
177	1090	B	1	H	1	48	0.48	0.48	1.560	1.5412
177	1090	D	1	H	1	14	0.14	0.48	1.519	1.5188
177	1090	B	1	H	1	50	0.5	0.5	1.556	1.5344
177	1090	D	1	H	1	16	0.16	0.5	1.480	1.5286
177	1090	B	1	H	1	52	0.52	0.52	1.557	1.534
177	1090	D	1	H	1	18	0.18	0.52	1.531	1.5312
177	1090	B	1	H	1	54	0.54	0.54	1.546	1.5452
177	1090	D	1	H	1	20	0.2	0.54	1.542	1.5422
177	1090	B	1	H	1	56	0.56	0.56	1.550	1.5414
177	1090	D	1	H	1	22	0.22	0.56	1.542	1.54
177	1090	B	1	H	1	58	0.58	0.58	1.527	1.5294
177	1090	D	1	H	1	24	0.24	0.58	1.539	1.5272
177	1090	B	1	H	1	60	0.6	0.6	1.489	1.5162
177	1090	D	1	H	1	26	0.26	0.6	1.539	1.525
177	1090	B	1	H	1	62	0.62	0.62	1.487	1.5132
177	1090	D	1	H	1	28	0.28	0.62	1.571	1.52
177	1090	B	1	H	1	64	0.64	0.64	1.480	1.5024
177	1090	D	1	H	1	30	0.3	0.64	1.523	1.5114
177	1090	B	1	H	1	66	0.66	0.66	1.451	1.4884
177	1090	D	1	H	1	32	0.32	0.66	1.532	1.5002
177	1090	B	1	H	1	68	0.68	0.68	1.456	1.4898
177	1090	D	1	H	1	34	0.34	0.68	1.539	1.5086
177	1090	B	1	H	1	70	0.7	0.7	1.471	1.4878
177	1090	D	1	H	1	36	0.36	0.7	1.545	1.5024
177	1090	B	1	H	1	72	0.72	0.72	1.428	1.4786
177	1090	D	1	H	1	38	0.38	0.72	1.529	1.495
177	1090	B	1	H	1	74	0.74	0.74	1.420	1.4686
177	1090	D	1	H	1	40	0.4	0.74	1.553	1.4898
177	1090	B	1	H	1	76	0.76	0.76	1.413	1.4662
177	1090	D	1	H	1	42	0.42	0.76	1.534	1.495
177	1090	B	1	H	1	78	0.78	0.78	1.411	1.4666
177	1090	D	1	H	1	44	0.44	0.78	1.564	1.4922
177	1090	B	1	H	1	80	0.8	0.8	1.411	1.4592
177	1090	D	1	H	1	46	0.46	0.8	1.541	1.4864
177	1090	B	1	H	1	82	0.82	0.82	1.369	1.4522
177	1090	D	1	H	1	48	0.48	0.82	1.547	1.481
177	1090	B	1	H	1	84	0.84	0.84	1.393	1.4496
177	1090	D	1	H	1	50	0.5	0.84	1.555	1.4878
177	1090	B	1	H	1	86	0.86	0.86	1.384	1.4616
177	1090	D	1	H	1	52	0.52	0.86	1.560	1.4966

Notes: From Gersonne, Hodell, Blum, et al. (1999). Only a portion of this table appears here. The complete table is available in [ASCII format](#).

Table T3. Shipboard dry density and water content values made on selected sediment core samples. (See table note. Continued on next two pages.)

Core, section, interval (cm)	Depth (mbsf)	Depth (mcd)	Water content (bulk)	Water content (dry)	Bulk density (g/cm ³)	Dry density (g/cm ³)	Grain density (g/cm ³)	Porosity (%)	Void Ratio
177-1090B-1H-1, 74-76	0.74	0.74	58.2	139.1	1.394	0.583	2.805	79.2	3.809
177-1090A-1H-1, 90-92	0.9	0.9	48.3	93.5	1.494	0.772	2.616	70.5	2.388
177-1090B-1H-2, 50-52	2	2	48.8	95.2	1.512	0.775	2.766	72	2.571
177-1090A-1H-2, 92-94	2.42	2.42	57.3	134	1.397	0.597	2.728	78.1	3.569
177-1090B-1H-3, 74-76	3.24	3.24	46.5	87	1.542	0.824	2.755	70.1	2.342
177-1090A-1H-3, 74-76	3.74	3.74	47.5	90.6	1.524	0.8	2.734	70.8	2.42
177-1090B-2H-1, 74-76	4.94	4.94	50.5	102.1	1.481	0.733	2.718	73	2.709
177-1090A-1H-4, 72-74	5.22	5.22	45.8	84.7	1.538	0.833	2.672	68.8	2.209
177-1090B-2H-2, 74-76	6.44	6.44	46.4	86.7	1.513	0.811	2.584	68.6	2.188
2H-3, 74-76	7.94	7.94	49.9	99.5	1.488	0.746	2.71	72.5	2.633
2H-4, 74-76	9.44	9.44	49	96.2	1.497	0.763	2.691	71.7	2.527
2H-5, 74-76	10.94	10.94	48	92.4	1.507	0.783	2.669	70.7	2.409
2H-6, 74-76	12.44	12.44	48.1	92.5	1.524	0.791	2.778	71.5	2.509
3H-1, 74-76	14.44	16.19	46.3	86.1	1.542	0.828	2.731	69.7	2.297
3H-1, 120-122	14.9	16.65	49.8	99.2	1.458	0.732	2.515	70.9	2.436
3H-2, 74-76	15.94	17.69	52.6	111.1	1.451	0.687	2.703	74.6	2.932
3H-3, 74-76	17.44	19.19	50.3	101.3	1.478	0.734	2.682	72.6	2.654
3H-4, 74-76	18.94	20.69	55.4	124	1.408	0.629	2.634	76.1	3.19
3H-5, 74-76	20.44	22.19	42.3	73.2	1.601	0.925	2.727	66.1	1.949
3H-6, 20-22	21.4	23.15	55.5	124.7	1.386	0.617	2.479	75.1	3.018
4H-2, 74-76	25.44	27.95	47.2	89.5	1.52	0.802	2.683	70.1	2.346
4H-3, 74-76	26.94	29.45	50.4	101.7	1.47	0.729	2.636	72.4	2.618
4H-3, 100-102	27.2	29.71	58.9	143.4	1.337	0.549	2.382	76.9	3.336
4H-4, 20-22	27.9	30.41	45.2	82.5	1.555	0.852	2.719	68.6	2.189
4H-5, 74-76	29.94	32.45	43.6	77.3	1.576	0.889	2.703	67.1	2.04
4H-6, 74-76	31.44	33.95	44.1	79	1.565	0.874	2.687	67.5	2.073
5H-2, 74-76	34.94	38.55	43.5	76.9	1.573	0.889	2.678	66.8	2.012
5H-3, 74-76	36.44	40.05	44.8	81.3	1.56	0.86	2.717	68.3	2.158
5H-4, 74-76	37.64	41.25	52.9	112.3	1.421	0.669	2.514	73.4	2.757
5H-5, 74-76	39.14	42.75	51.6	106.6	1.459	0.706	2.668	73.5	2.778
5H-6, 74-76	40.64	44.25	42.6	74.3	1.588	0.911	2.689	66.1	1.951
6H-1, 74-76	42.94	46.55	44.8	81	1.565	0.865	2.738	68.4	2.167
6H-2, 74-76	44.44	48.05	41.5	71	1.615	0.944	2.737	65.5	1.898
6H-3, 74-76	45.94	49.55	45.2	82.5	1.524	0.835	2.554	67.3	2.057
6H-4, 74-76	47.44	51.05	50.6	102.4	1.47	0.726	2.657	72.7	2.659
6H-5, 74-76	48.94	52.55	44.8	81.1	1.552	0.857	2.665	67.8	2.11
6H-6, 74-76	50.44	54.05	47.3	89.7	1.495	0.788	2.544	69	2.228
7H-2, 74-76	53.94	60.24	39.6	65.7	1.607	0.97	2.566	62.2	1.647
7H-3, 74-76	55.44	61.74	40.5	68	1.627	0.969	2.716	64.3	1.804
7H-4, 74-76	56.94	63.24	42.1	72.8	1.595	0.923	2.687	65.7	1.911
7H-5, 74-76	58.44	64.74	38.6	62.8	1.653	1.016	2.69	62.2	1.649
8H-1, 74-76	61.94	65.65	46.2	85.8	1.531	0.824	2.66	69	2.228
8H-2, 22-24	62.92	66.63	46.4	86.6	1.529	0.819	2.67	69.3	2.258
8H-2, 122-124	63.92	67.63	44.6	80.6	1.558	0.862	2.687	67.9	2.116
8H-3, 74-76	64.94	68.65	42.9	75	1.561	0.892	2.572	65.3	1.885
8H-4, 74-76	66.44	70.15	66.4	197.9	1.288	0.433	2.636	83.6	5.093
8H-4, 124-126	66.94	70.65	53.8	116.4	1.442	0.667	2.748	75.7	3.123
8H-5, 74-76	67.94	71.65	61.4	159.4	1.327	0.511	2.508	79.6	3.903
9H-3, 94-96	74.64	78.33	56.6	130.3	1.401	0.608	2.692	77.4	3.426
9H-4, 74-76	75.94	79.63	53.9	116.8	1.423	0.657	2.612	74.9	2.978
9H-5, 74-76	77.44	81.13	52.9	112.1	1.456	0.687	2.765	75.2	3.028
9H-6, 74-76	78.94	82.63	59	144.1	1.374	0.563	2.71	79.2	3.813
10H-1, 122-124	81.42	85.99	49.1	96.3	1.5	0.764	2.714	71.8	2.552
10H-2, 22-24	81.92	86.49	57	132.7	1.369	0.588	2.478	76.3	3.213

Table T3 (continued).

Core, section, interval (cm)	Depth (mbsf)	Depth (mcd)	Water content (bulk)	Water content (dry)	Bulk density (g/cm ³)	Dry density (g/cm ³)	Grain density (g/cm ³)	Porosity (%)	Void Ratio
177-1090B-									
10H-2, 72-74	82.42	86.99	47.3	89.7	1.531	0.807	2.754	70.7	2.411
10H-3, 74-76	83.94	88.51	54	117.6	1.426	0.655	2.646	75.2	3.038
10H-4, 74-76	85.44	90.01	59	143.9	1.368	0.561	2.645	78.8	3.719
10H-5, 74-76	86.94	91.51	53.1	113.4	1.427	0.669	2.576	74	2.852
11H-1, 110-112	90.8	94.79	54.3	119	1.434	0.654	2.737	76.1	3.182
11H-2, 74-76	91.94	95.93	57.5	135.3	1.385	0.588	2.646	77.8	3.496
11H-3, 74-76	93.44	97.43	58.7	142.4	1.369	0.565	2.627	78.5	3.653
11H-4, 74-76	94.94	98.93	55	122.3	1.398	0.629	2.529	75.1	3.021
11H-5, 22-24	95.92	99.91	54.9	121.5	1.419	0.641	2.673	76	3.172
11H-6, 18-20	96.78	100.77	60.8	155.2	1.343	0.527	2.603	79.8	3.944
11H-7, 46-48	98.56	102.55	50.2	101	1.476	0.734	2.661	72.4	2.624
12H-1, 74-76	99.94	103.61	43	75.5	1.553	0.885	2.545	65.2	1.875
12H-2, 74-76	101.44	105.11	48.1	92.6	1.503	0.781	2.653	70.6	2.399
12H-3, 74-76	102.94	106.61	44.5	80	1.56	0.867	2.687	67.7	2.101
12H-4, 74-76	104.44	108.11	44.4	80	1.556	0.864	2.663	67.5	2.081
12H-5, 74-76	105.94	109.61	42.2	72.9	1.568	0.906	2.558	64.6	1.822
12H-6, 74-76	107.44	111.11	52.2	109.1	1.447	0.692	2.632	73.7	2.803
13H-1, 74-76	109.44	114.85	58.2	139.4	1.369	0.572	2.578	77.8	3.51
13H-2, 74-76	110.94	116.35	61.9	162.7	1.324	0.504	2.535	80.1	4.027
13H-3, 74-76	112.44	117.85	62.3	165.4	1.3	0.49	2.351	79.2	3.798
13H-4, 74-76	113.94	119.35	57.9	137.5	1.375	0.579	2.604	77.8	3.496
13H-5, 74-76	115.44	120.85	62.1	163.9	1.321	0.501	2.522	80.1	4.037
13H-6, 50-52	116.7	122.11	58.2	139	1.368	0.572	2.569	77.7	3.488
14H-2, 74-76	120.44	124.09	60.3	151.7	1.328	0.528	2.419	78.2	3.584
14H-3, 74-76	121.94	125.59	53.7	115.9	1.431	0.663	2.65	75	2.999
14H-4, 74-76	123.44	127.09	58.8	142.8	1.362	0.561	2.577	78.2	3.595
14H-5, 74-76	124.94	128.59	62.8	168.6	1.316	0.49	2.531	80.6	4.167
14H-6, 74-76	126.44	130.09	53.9	117	1.399	0.645	2.445	73.6	2.794
15H-1, 120-122	128.9	135.39	60.3	152	1.348	0.535	2.596	79.4	3.854
15H-2, 74-76	129.94	136.43	56.2	128.5	1.396	0.611	2.614	76.6	3.28
15H-3, 74-76	131.44	137.93	55.8	126.4	1.4	0.618	2.612	76.3	3.223
15H-4, 74-76	132.94	139.43	43.2	76.2	1.553	0.881	2.558	65.5	1.902
15H-5, 74-76	134.44	140.93	47.2	89.3	1.52	0.803	2.679	70	2.336
16H-1, 74-76	137.94	144.59	54.7	120.7	1.417	0.642	2.641	75.7	3.112
16H-2, 120-122	139.9	146.55	57.6	135.9	1.377	0.584	2.592	77.5	3.442
16H-3, 74-76	140.94	147.59	52.9	112.5	1.414	0.665	2.471	73.1	2.713
16H-4, 74-76	142.44	149.09	49.3	97.3	1.487	0.754	2.657	71.6	2.524
16H-5, 74-76	143.94	150.59	56.9	132	1.377	0.594	2.528	76.5	3.258
16H-6, 22-24	144.92	151.57	60.9	155.9	1.326	0.518	2.456	78.9	3.74
17H-1, 122-124	147.92	155.42	54.2	118.1	1.423	0.652	2.634	75.2	3.039
17H-2, 74-76	148.94	156.44	55.2	123.4	1.405	0.629	2.601	75.8	3.135
17H-3, 74-76	150.44	157.94	51.5	106	1.466	0.711	2.7	73.7	2.796
17H-4, 74-76	151.94	159.44	57	132.5	1.37	0.589	2.482	76.3	3.211
17H-5, 34-36	153.04	160.54	57.1	133	1.369	0.588	2.48	76.3	3.22
18H-1, 122-124	157.42	165.2	59.2	145.4	1.362	0.555	2.615	78.8	3.712
18H-2, 22-24	157.92	165.7	56.2	128.1	1.397	0.613	2.619	76.6	3.276
18H-2, 74-76	158.44	166.22	56.5	129.6	1.384	0.603	2.542	76.3	3.219
18H-3, 22-24	159.42	167.2	57.9	137.3	1.345	0.567	2.361	76	3.165
18H-4, 72-74	161.42	169.2	57.1	133.2	1.383	0.593	2.595	77.1	3.375
18H-5, 74-76	162.94	170.72	58.7	142	1.363	0.563	2.576	78.1	3.572
18H-6, 74-76	164.44	172.22	58.3	139.9	1.359	0.566	2.505	77.4	3.422
19H-1, 60-62	166.3	175.79	60.5	153.4	1.328	0.524	2.44	78.5	3.656
19H-2, 74-76	167.94	177.43	60.9	155.6	1.318	0.515	2.379	78.3	3.615
19H-3, 86-88	169.56	179.05	49.5	98.2	1.476	0.745	2.607	71.4	2.499
19H-4, 72-74	170.92	180.41	58.1	138.4	1.357	0.569	2.47	77	3.34
19H-5, 72-74	172.42	181.91	57	132.7	1.376	0.591	2.53	76.6	3.28
20H-1, 72-74	175.92	183.53	58.8	142.9	1.355	0.558	2.518	77.8	3.514
20H-2, 122-124	177.92	185.53	58.4	140.5	1.357	0.565	2.502	77.4	3.432
20H-3, 74-76	178.94	186.55	59.1	144.8	1.334	0.545	2.373	77	3.356
20H-4, 74-76	180.44	188.05	60.3	152.1	1.327	0.526	2.411	78.2	3.581
20H-5, 74-76	181.94	189.55	56.3	128.8	1.383	0.605	2.523	76	3.172
20H-6, 74-76	183.44	191.05	55.6	125.1	1.36	0.604	2.303	73.8	2.813
21X-1, 74-76	185.44	193.49	63.5	174.2	1.275	0.465	2.227	79.1	3.787
21X-2, 50-52	186.7	194.75	67	202.6	1.244	0.411	2.205	81.4	4.362
21X-2, 120-122	187.4	195.45	59.9	149.2	1.338	0.537	2.462	78.2	3.586
21X-3, 74-76	188.44	196.49	59.4	146.5	1.341	0.544	2.456	77.8	3.514
21X-4, 74-76	189.94	197.99	60.3	151.8	1.334	0.53	2.465	78.5	3.655

Table T3 (continued).

Core, section, interval (cm)	Depth (mbsf)	Depth (mcd)	Water content (bulk)	Water content (dry)	Bulk density (g/cm ³)	Dry density (g/cm ³)	Grain density (g/cm ³)	Porosity (%)	Void Ratio
177-1090B-									
21X-5, 74-76	191.44	199.49	61.9	162.8	1.307	0.497	2.378	79.1	3.781
21X-6, 74-76	192.94	200.99	56.9	132.1	1.356	0.584	2.374	75.4	3.063
22X-1, 74-76	195.14	202.75	62	163.1	1.292	0.491	2.253	78.2	3.59
22X-2, 74-76	196.64	204.25	56.5	129.8	1.383	0.602	2.54	76.3	3.22
22X-3, 74-76	198.14	205.75	62.3	165	1.312	0.495	2.447	79.8	3.942
22X-4, 74-76	199.64	207.25	64.9	184.8	1.278	0.449	2.355	81	4.25
22X-5, 74-76	201.14	208.75	69.9	232.1	1.206	0.363	2.049	82.3	4.644
22X-6, 74-76	202.64	210.25	62.5	166.8	1.316	0.493	2.506	80.3	4.082
23X-1, 74-76	204.84	213.24	57.5	135.3	1.388	0.59	2.672	77.9	3.529
23X-3, 74-76	207.84	216.24	49.6	98.4	1.478	0.745	2.624	71.6	2.521
23X-5, 74-76	209.74	218.14	49	96.1	1.491	0.761	2.655	71.3	2.49
23X-7, 74-76	212.74	221.14	51.3	105.2	1.451	0.707	2.584	72.6	2.653
26X-3, 21-23	236.41	248.4	62.9	169.3	1.312	0.487	2.504	80.5	4.141
26X-5, 22-24	239.42	251.41	59.5	146.7	1.358	0.55	2.601	78.8	3.727
26X-7, 16-18	242.36	254.35	65.3	187.9	1.277	0.444	2.389	81.4	4.383
27X-1, 96-98	243.86	255.85	62.2	164.5	1.308	0.494	2.402	79.4	3.858
27X-2, 97-99	245.37	257.36	57.9	137.6	1.368	0.576	2.545	77.4	3.421
27X-4, 100-102	248.4	260.39	58.1	138.9	1.374	0.575	2.617	78	3.551
28X-3, 28-30	255.88	267.87	58.2	139.4	1.372	0.573	2.612	78.1	3.556
28X-4, 92-94	258.02	270.01	67.5	207.6	1.257	0.409	2.381	82.8	4.829
28X-7, 34-36	261.94	273.93	71	244.3	1.236	0.359	2.495	85.6	5.951
29X-1, 44-46	262.74	274.73	66.5	198.2	1.268	0.425	2.402	82.3	4.647
29X-3, 21-23	265.51	277.5	73.6	278.7	1.204	0.318	2.362	86.5	6.428
29X-5, 108-110	269.38	281.37	67.9	211.3	1.259	0.404	2.439	83.4	5.033
30X-1, 124-126	273.24	285.23	59.5	146.8	1.37	0.555	2.719	79.6	3.899
30X-3, 20-22	275.2	287.19	66.7	200.5	1.259	0.419	2.334	82.1	4.571
30X-6, 30-32	279.8	291.79	61.7	161.4	1.318	0.504	2.458	79.5	3.875
30X-6, 122-124	280.72	292.71	70.5	239.2	1.231	0.363	2.379	84.7	5.556
31X-3, 65-67	285.35	297.34	55.9	126.7	1.392	0.614	2.559	76	3.167
31X-4, 72-74	286.92	298.91	60.9	156					

Note: From Gersonde, Hodell, Blum, et al. (1999).

Table T4. Shipboard spectral reflectance values given as percent reflectance in 100-nm intervals.

Site	Hole	Core	Type	Section	Interval (cm)		Depth (mbsf)	Depth (mcd)	Age (Ma)	250–350 nm	450–550 nm	650–750 nm	850–950 nm
					Top	Bottom							
1090	A	1	H	1	5	7	0.06	0.06	0.1516	61.53	23.07	55.46	63.34
1090	A	1	H	1	9	11	0.1	0.1	0.1524	-9.99	37.83	54.5	63.16
1090	A	1	H	1	13	15	0.14	0.14	0.1531	41.52	39.83	42.79	63.8
1090	A	1	H	1	17	19	0.18	0.18	0.1539	42.37	38.91	56.68	65.4
1090	A	1	H	1	21	23	0.22	0.22	0.1547	-9.99	39.71	57.21	65.39
1090	A	1	H	1	25	27	0.26	0.26	0.1554	63.35	41.39	44.74	66.74
1090	A	1	H	1	29	31	0.3	0.3	0.1562	36.99	39.31	57.26	65.82
1090	A	1	H	1	33	35	0.34	0.34	0.1570	80.25	45.4	66.59	76.41
1090	A	1	H	1	37	39	0.38	0.38	0.1577	38.01	38.37	55.36	63.84
1090	A	1	H	1	41	43	0.42	0.42	0.1585	68.52	47.94	67.95	76.09
1090	A	1	H	1	45	47	0.46	0.46	0.1592	47.39	21.46	41.26	61.43
1090	A	1	H	1	49	51	0.5	0.5	0.1600	53.86	43.38	64.46	74.47
1090	A	1	H	1	53	55	0.54	0.54	0.1608	47.67	32.4	49.75	58.52
1090	A	1	H	1	57	59	0.58	0.58	0.1615	53.72	33.89	49.77	57.72
1090	A	1	H	1	61	63	0.62	0.62	0.1623	49.91	41.82	46.76	68.97
1090	A	1	H	1	65	67	0.66	0.66	0.1630	67.14	35.78	52.1	59.72
1090	A	1	H	1	69	71	0.7	0.7	0.1638	52.43	39.3	54.84	63.02
1090	A	1	H	1	73	75	0.74	0.74	0.1646	40.86	41.65	56.67	65
1090	A	1	H	1	77	79	0.78	0.78	0.1653	45.91	42.65	57.97	64.37
1090	A	1	H	1	81	83	0.82	0.82	0.1661	71.78	38.35	58.9	68.97
1090	A	1	H	1	85	87	0.86	0.86	0.1669	48.94	37.77	55.93	64.48
1090	A	1	H	1	89	91	0.9	0.9	0.1676	68.51	37.24	55.85	65.78
1090	A	1	H	1	93	95	0.94	0.94	0.1684	59.63	32.16	51.67	61.38
1090	A	1	H	1	97	99	0.98	0.98	0.1691	59.33	32.16	49.31	58.76
1090	A	1	H	1	101	103	1.02	1.02	0.1699	29.4	42.48	62.97	71.92
1090	A	1	H	1	105	107	1.06	1.06	0.1707	64.54	34.44	52.84	61.11
1090	A	1	H	1	109	111	1.1	1.1	0.1714	31.65	37.98	57.46	65.9
1090	A	1	H	1	113	115	1.14	1.14	0.1722	23.56	36.23	54.13	61.54
1090	A	1	H	1	117	119	1.18	1.18	0.1730	38.92	31.7	51.12	59.69
1090	A	1	H	1	121	123	1.22	1.22	0.1737	35.94	30.48	49.05	57.84
1090	A	1	H	1	125	127	1.26	1.26	0.1745	47.88	32.49	51.4	50.16
1090	A	1	H	1	129	131	1.3	1.3	0.1752	19.31	22.75	41.23	49.86
1090	A	1	H	1	133	135	1.34	1.34	0.1760	51.62	22.63	41.4	50.45
1090	A	1	H	1	137	139	1.38	1.38	0.1768	36.9	25.57	45.94	54.83
1090	A	1	H	1	141	143	1.42	1.42	0.1775	60.51	25.98	43.09	50.16
1090	A	1	H	1	145	147	1.46	1.46	0.1783	66.11	28.16	45.05	51.25
1090	A	1	H	1	147	149	1.48	1.48	0.1787	-9.99	30.89	46.93	52.48
1090	A	1	H	2	5	7	1.56	1.56	0.1802	52.97	27.34	42.19	47.79
1090	A	1	H	2	9	11	1.6	1.6	0.1810	20.24	28.1	43.93	49.52
1090	A	1	H	2	13	15	1.64	1.64	0.1817	48.94	21.42	40.6	46.58
1090	A	1	H	2	17	19	1.68	1.68	0.1825	36.8	23.67	37.85	42.89
1090	A	1	H	2	21	23	1.72	1.72	0.1832	47.09	26.88	44.42	50.07
1090	A	1	H	2	25	27	1.76	1.76	0.1840	52.56	11.47	36.97	43.62
1090	A	1	H	2	29	31	1.8	1.8	0.1848	72.4	25.92	28.72	44.97
1090	A	1	H	2	33	35	1.84	1.84	0.1855	42.37	21.52	25.81	41.73
1090	A	1	H	2	37	39	1.88	1.88	0.1863	23.56	21.6	24.04	38.96
1090	A	1	H	2	41	43	1.92	1.92	0.1870	53.86	20.49	32.54	39.35
1090	A	1	H	2	45	47	1.96	1.96	0.1878	33.52	22.84	36.29	43.76
1090	A	1	H	2	49	51	2	2	0.1886	27.48	19.89	23.74	38.81
1090	A	1	H	2	53	55	2.04	2.04	0.1893	41.89	18.63	30.23	29.83
1090	A	1	H	2	57	59	2.08	2.08	0.1901	53.47	19.47	25.68	26.03
1090	A	1	H	2	61	63	2.12	2.12	0.1909	50	21.91	26.74	25.97
1090	A	1	H	2	65	67	2.16	2.16	0.1916	69.95	19.5	24.37	24.05
1090	A	1	H	2	69	71	2.2	2.2	0.1924	-104.02	19.56	23.83	24.18
1090	A	1	H	2	73	75	2.24	2.24	0.1931	44.51	25.97	32.2	33.72
1090	A	1	H	2	77	79	2.28	2.28	0.1939	14.56	19.58	24.66	25.06
1090	A	1	H	2	81	83	2.32	2.32	0.1947	5.32	24.49	31.38	31.13
1090	A	1	H	2	85	87	2.36	2.36	0.1954	31.65	20.8	25.64	25.43
1090	A	1	H	2	89	91	2.4	2.4	0.1962	-2.83	21.18	26.78	26.93
1090	A	1	H	2	93	95	2.44	2.44	0.1970	63.11	23.81	22.67	29.18
1090	A	1	H	2	97	99	2.48	2.48	0.1977	45.98	22.57	26.3	25.53
1090	A	1	H	2	101	103	2.52	2.52	0.1985	38.92	21.88	27.99	28.72

Notes: From Gersonde, Hodell, Blum, et al. (1999). Only a portion of this table appears here. The complete table is available in [ASCII format](#).

Table T5. Weight percent CaCO₃ values.

Leg	Site Hole	Core	Type	Section	Interval (cm)		Depth (mbsf)	Depth (mcd)	Age (Ma)	CaCO ₃ (wt%)	
					Top	Bottom					
177	1090	B	1	H	1	74	75	0.74	0.74	0.165	52.3
177	1090	D	1	H	2	33	34	1.83	2.17	0.192	61.004
177	1090	D	1	H	2	37	38	1.87	2.21	0.193	60.051
177	1090	D	1	H	2	41	42	1.91	2.25	0.193	65.143
177	1090	D	1	H	2	45	46	1.95	2.29	0.194	67.416
177	1090	D	1	H	2	49	50	1.99	2.33	0.195	68.923
177	1090	D	1	H	2	53	54	2.03	2.37	0.196	71.686
177	1090	D	1	H	2	57	58	2.07	2.41	0.196	78.198
177	1090	D	1	H	2	61	62	2.11	2.45	0.197	77.714
177	1090	D	1	H	2	65	66	2.15	2.49	0.198	78.546
177	1090	D	1	H	2	69	70	2.19	2.53	0.199	80.065
177	1090	D	1	H	2	73	74	2.23	2.57	0.199	80.953
177	1090	D	1	H	2	77	78	2.27	2.61	0.200	82.049
177	1090	D	1	H	2	81	82	2.31	2.65	0.201	82.021
177	1090	D	1	H	2	85	86	2.35	2.69	0.202	87.267
177	1090	D	1	H	2	89	90	2.39	2.73	0.202	87.395
177	1090	D	1	H	2	93	94	2.43	2.77	0.203	85.878
177	1090	D	1	H	2	97	98	2.47	2.81	0.204	77.800
177	1090	D	1	H	2	101	102	2.51	2.85	0.205	86.120
177	1090	D	1	H	2	105	106	2.55	2.89	0.206	81.670
177	1090	D	1	H	2	109	110	2.59	2.93	0.206	76.784
177	1090	D	1	H	2	113	114	2.63	2.97	0.207	79.934
177	1090	D	1	H	2	117	118	2.67	3.01	0.208	81.722
177	1090	D	1	H	2	121	122	2.71	3.05	0.209	82.287
177	1090	D	1	H	2	125	126	2.75	3.09	0.209	82.299
177	1090	D	1	H	2	129	130	2.79	3.13	0.210	84.089
177	1090	D	1	H	2	133	134	2.83	3.17	0.211	83.745
177	1090	D	1	H	2	137	138	2.87	3.21	0.212	83.278
177	1090	B	1	H	3	74	75	3.24	3.24	0.212	85.6
177	1090	D	1	H	2	141	142	2.91	3.25	0.212	80.134
177	1090	D	1	H	2	145	146	2.95	3.29	0.213	84.073
177	1090	D	1	H	2	147	148	2.97	3.31	0.214	83.256
177	1090	D	1	H	3	5	6	3.05	3.39	0.215	78.348
177	1090	D	1	H	3	9	10	3.09	3.43	0.216	81.873
177	1090	D	1	H	3	13	14	3.13	3.47	0.217	82.849
177	1090	D	1	H	3	17	18	3.17	3.51	0.217	79.376
177	1090	D	1	H	3	21	22	3.21	3.55	0.218	80.950
177	1090	D	1	H	3	25	26	3.25	3.59	0.219	82.727
177	1090	D	1	H	3	29	30	3.29	3.63	0.220	80.478
177	1090	D	1	H	3	33	34	3.33	3.67	0.220	86.627
177	1090	D	1	H	3	37	38	3.37	3.71	0.221	85.761
177	1090	D	1	H	3	41	42	3.41	3.75	0.222	84.649
177	1090	D	1	H	3	45	46	3.45	3.79	0.223	85.518
177	1090	D	1	H	3	49	50	3.49	3.83	0.223	87.129
177	1090	D	1	H	3	53	54	3.53	3.87	0.224	85.833
177	1090	D	1	H	3	57	58	3.57	3.91	0.225	85.025
177	1090	D	1	H	3	61	62	3.61	3.95	0.226	84.413
177	1090	D	1	H	3	65	66	3.65	3.99	0.226	84.469
177	1090	D	1	H	3	69	70	3.69	4.03	0.227	82.907
177	1090	D	1	H	3	73	74	3.73	4.07	0.228	81.950
177	1090	D	1	H	3	77	78	3.77	4.11	0.229	84.159
177	1090	D	1	H	3	81	82	3.81	4.15	0.230	81.768
177	1090	D	1	H	3	85	86	3.85	4.19	0.230	83.082
177	1090	D	1	H	3	89	90	3.89	4.23	0.231	79.700
177	1090	D	1	H	3	93	94	3.93	4.27	0.232	79.026
177	1090	D	1	H	3	97	98	3.97	4.31	0.233	78.827
177	1090	D	1	H	3	101	102	4.01	4.35	0.233	78.366
177	1090	D	1	H	3	105	106	4.05	4.39	0.234	77.547
177	1090	D	1	H	3	109	110	4.09	4.43	0.235	77.333
177	1090	D	1	H	3	113	114	4.13	4.47	0.236	73.980
177	1090	D	1	H	3	117	118	4.17	4.51	0.236	70.248
177	1090	D	1	H	3	121	122	4.21	4.55	0.237	70.148
177	1090	D	1	H	3	125	126	4.25	4.59	0.238	70.488
177	1090	D	1	H	3	129	130	4.29	4.63	0.239	67.120

Note: Only a portion of this table appears here. The complete table is available in [ASCII format](#).